Supplementary Information

NES consensus redefined by structures of PKI-type and Rev-type nuclear export signals bound to CRM1

Thomas Güttler [1,5], Tobias Madl [2,3,5], Piotr Neumann [4,5], Danilo Deichsel [1],

Lorenzo Corsini [2,3], Thomas Monecke [4], Ralf Ficner [4], Michael Sattler [2,3] & Dirk Görlich [1]

[1] Max-Planck-Institut für Biophysikalische Chemie, Am Fassberg 11, 37077 Göttingen, Germany.

[2] Institute of Structural Biology, Helmholtz Zentrum München, Ingolstädter Landstr. 1, 85746 Neuherberg, Germany.

[3] Munich Center for Integrated Protein Science at Department Chemie, Technische Universität München, Lichtenbergstr. 4, 85747 Garching, Germany.

[4] Abteilung für Molekulare Strukturbiologie, GZMB, Georg-August-Universität Göttingen, Justus-von-Liebig-Weg 11, 37077 Göttingen, Germany.

[5] These authors contributed equally to this work.

Correspondence should be addressed to D.G. (goerlich@mpibpc.mpg.de).

Supplementary Results

Supplementary Figures 1-7

Supplementary Table 1

Supplementary Methods

Supplementary References

Nature Structural & Molecular Biology: doi:10.1038/nsmb.1931

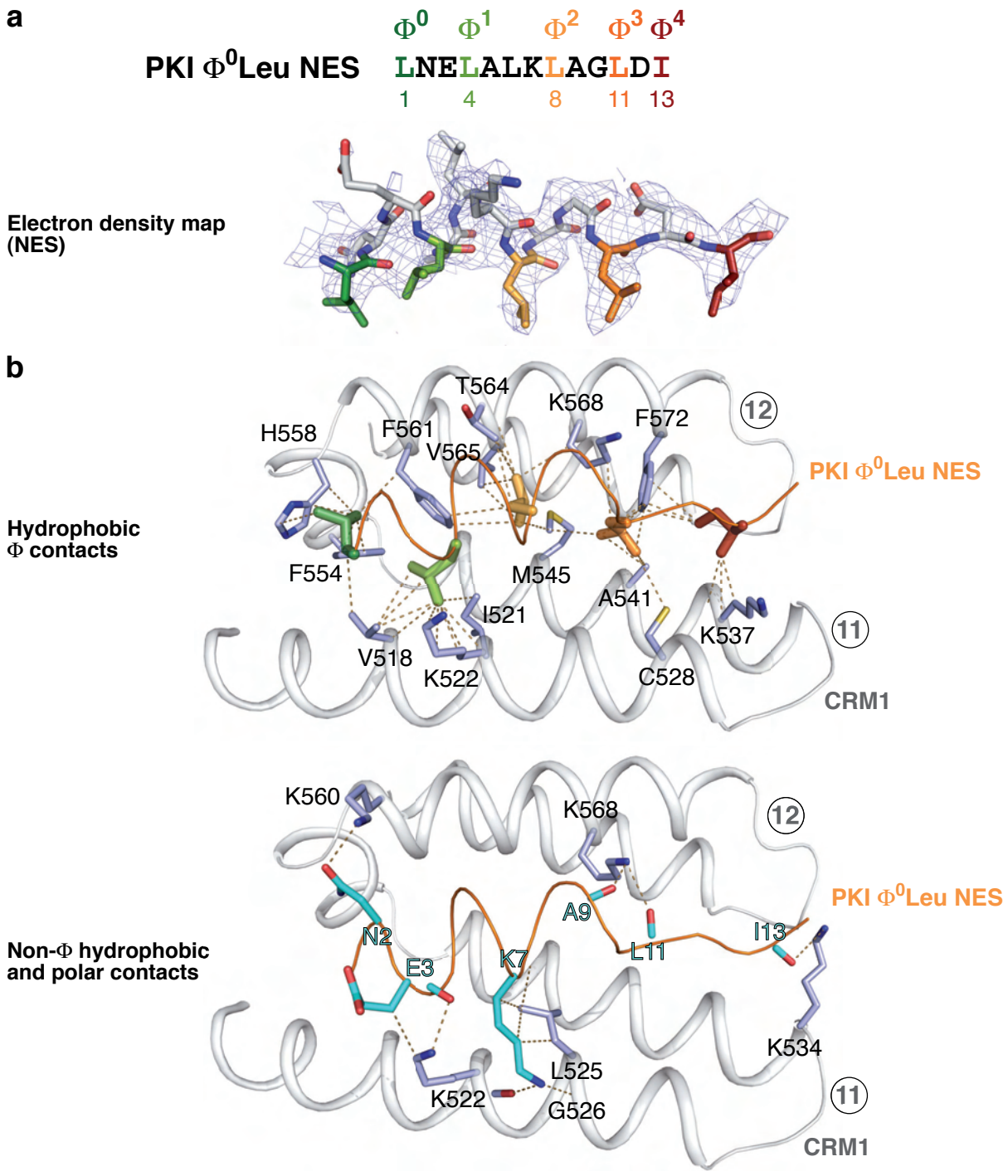

Supplementary Figure 1 Details of the PKI Φ^0Leu NES·CRM1 interaction (related to **Fig. 2**).

(a) Upper: Sequence of the PKI Φ^0Leu NES. Φ residues are colored according to **Figure 1a**. **Lower:** Panel displays the 2Fo-Fc electron density map (blue mesh, contoured at 1.0 σ) for the PKI Φ^0Leu NES (shown as sticks) in the chimeric RanGTP·CRM1·NES complex. Φ residues are colored according to the shown sequence. Note that all Φ residues are well defined in the map. In all panels, dark blue marks nitrogen, oxygen is shown in light red and sulfur is colored in yellow.

(b) CRM1 HEAT repeats 11-12 (gray cartoon) are shown with the NES peptide bound (backbone traced in orange). NES-binding residues of CRM1 are depicted as blue sticks. Dashed lines link interacting atoms. Lines pointing onto backbones indicate contacts to carbonyl-carbons or amide groups. **Upper:** Panel shows the hydrophobic contacts of the Φ residues (distance ≤ 4.0 Å). The respective Φ residues are shown as sticks, the color code is explained in **a**. **Lower:** Panel shows the non-Φ hydrophobic (distance ≤ 4.0 Å) as well as polar (distance ≤ 3.8 Å) contacts of NES residues (cyan sticks).

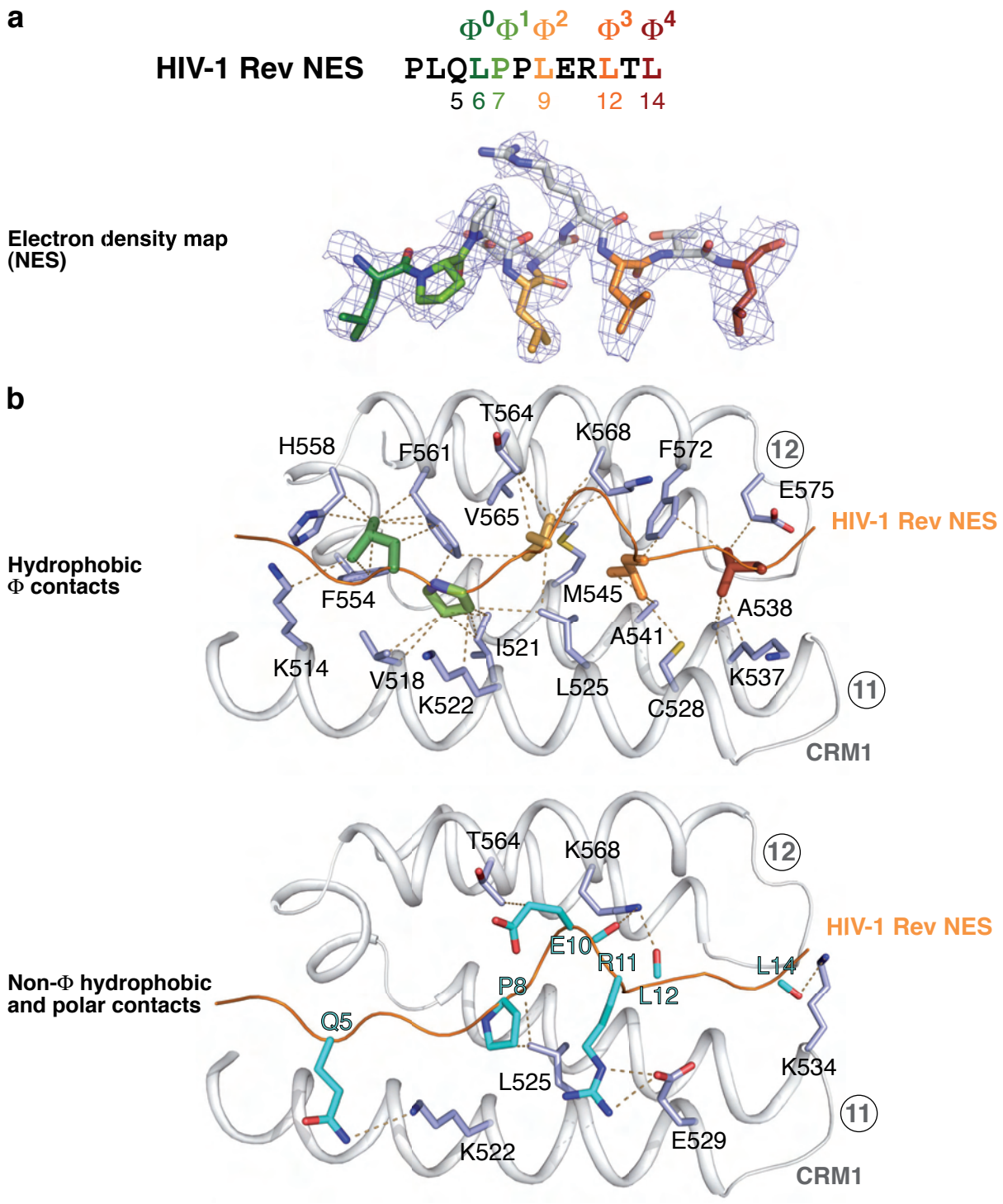

Supplementary Figure 2 Details of the HIV-1 Rev NES·CRM1 interaction (related to **Fig. 7**).

For explanation, see **Supplementary Figure 1**.

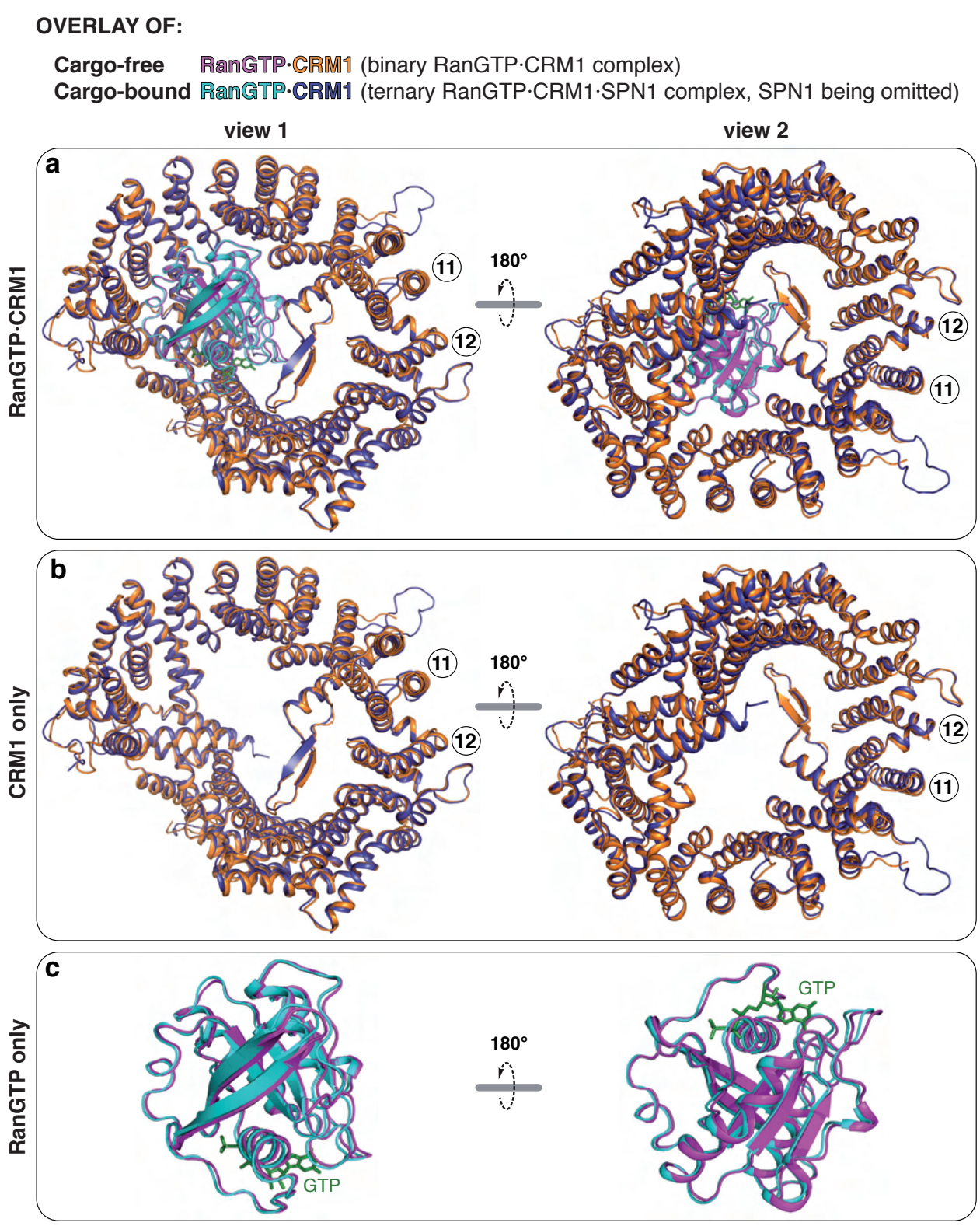

Supplementary Figure 3 Comparison of the overall structures of RanGTP·CRM1 from the binary (cargo-free) RanGTP·CRM1 complex and the ternary RanGTP·CRM1·SPN1 complex (PDB-ID 3GJX, chains F and D, ref. 1). This figure is related to **Figure 7**.

(a) Pictures show an overlay of RanGTP·CRM1 from the indicated complexes (in cartoon representation). The color code is explained on top of the figure. The overlay is based on a Cα alignment of the CRM1 molecules (RMSD = 0.843 Å). HEAT repeats forming the hydrophobic cleft (11 and 12) are labeled.

(b) As in **a**, but here RanGTP was omitted for clarity.

(c) As in **a**, but here CRM1 was omitted and Ran was enlarged. GTP is shown for orientation (green sticks).

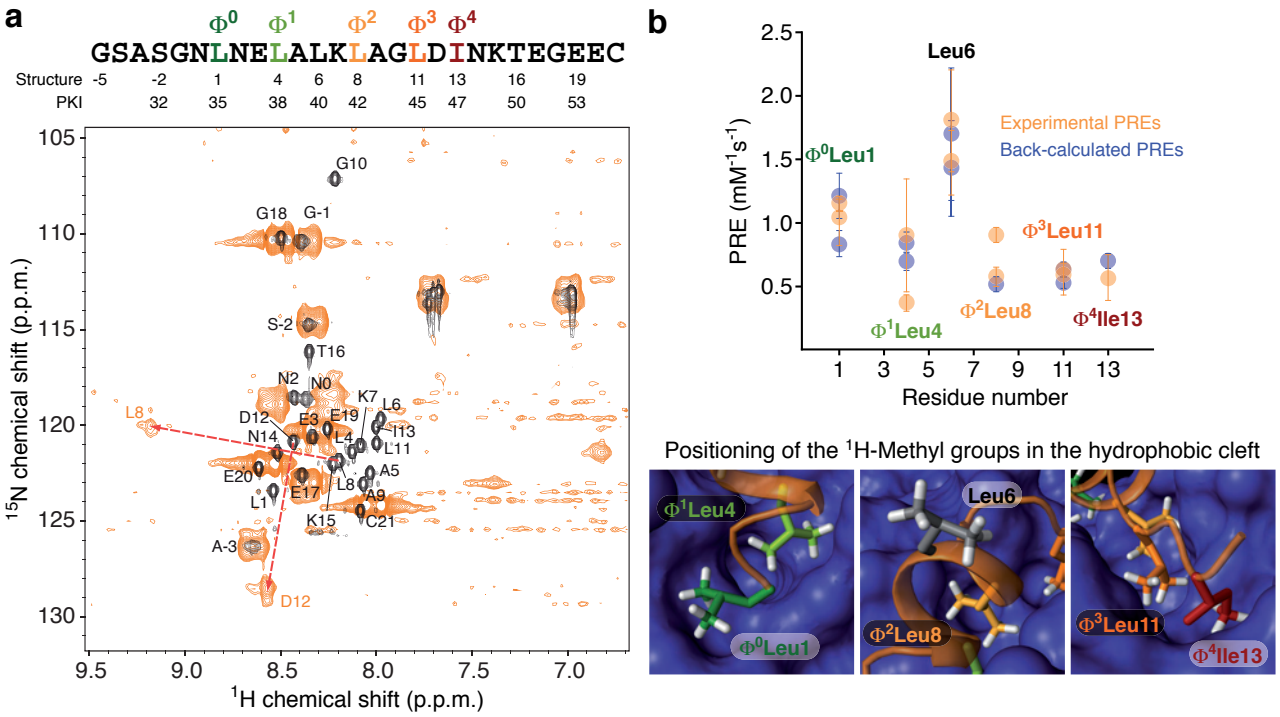

Supplementary Figure 4 NMR-spectroscopic analysis of the free and CRM1·RanGTP-bound PKI Φ^0Leu NES (related to **Fig. 3**).

(a) Overlay of the ^{1}H,^{15}N-HSQC NMR spectrum of the unbound PKI NES peptide (black) and the ^{1}H,^{15}N-CRINEPT-HMQC spectrum of the PKI NES peptide in the export complex (orange). Signals are labeled according to the shown residue numbers ("structure"). Arrows indicate changes in the chemical shift of selected residues that occur when the NES is incorporated in the export complex.

(b) Upper: Diagram shows solvent PRE (paramagnetic relaxation enhancement) data for the CRM1-bound NES. PRE values positively correlate with the solvent-accessibility of methyl groups. Experimental (orange) and back-calculated ^{1}H PREs (blue) for methyl groups are displayed. **Lower:** The panels show how the ^{1}H-methyl groups of the indicated residues are positioned in the hydrophobic cleft of CRM1. The backbone of the PKI NES is shown in orange, side chains are color-coded as in **Figure 3b**, protons are colored in light gray. CRM1 is shown as a surface representation (blue).

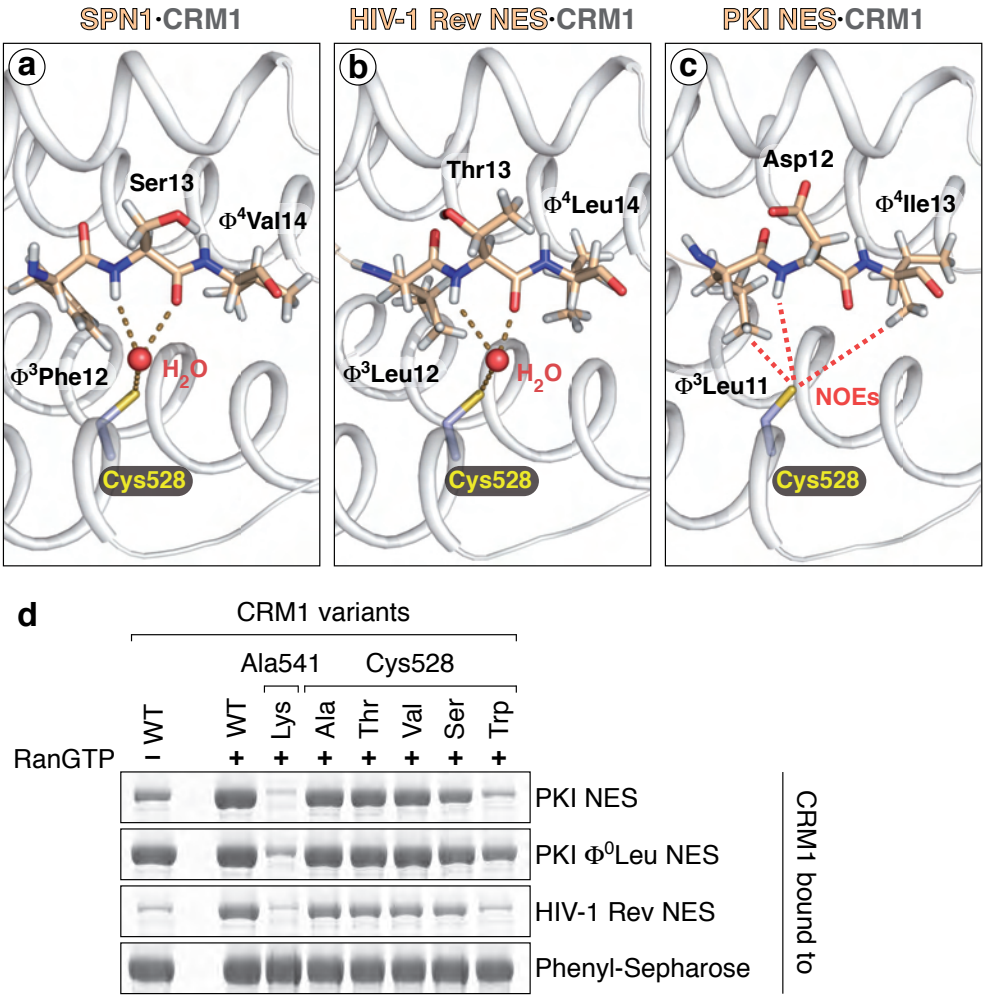

Supplementary Figure 5 Evidence for a hydrogen bonding network involving CRM1-Cys528 and NES peptide backbones (related to **Figs. 2, 3, 7**).

Panels **a**-**c** show cartoon representations of CRM1 (gray) and the indicated ligand (light orange), focussing on the region around CRM1-Cys528. Selected residues are depicted as sticks (with oxygen in red, nitrogen in blue, sulfur in yellow and protons in gray). The higher-resolution structures of the SPN1 (PDB-ID 3GJX, ref. 1) and HIV-1 Rev NES complexes revealed a conspicuous water molecule (red sphere) in the vicinity of CRM1-Cys528.

(a) The dashed lines illustrate the hydrogen bonding network that involves this water molecule, CRM1-Cys528 and the backbone of SPN1-Ser13.

(b) The panel illustrates the analogous hydrogen bonding network for the HIV-1 Rev NES·CRM1·RanGTP complex.

(c) The PKI Φ^0Leu NES·CRM1·RanGTP electron density map could not resolve water molecules. However, we observed NOE cross peaks for a cysteine sulfhydryl protected against solvent exchange (**Fig. 3c**), typical for stable hydrogen bonding interactions. This cysteine can be assigned to CRM1-Cys528, which is located in the vicinity of the PKI Φ^0Leu NES peptide (panel **d**) and is the only cysteine within the hydrophobic cleft. Thus, the NOE pattern (cross peaks between CRM1-Cys528 Hγ and side chain methyl protons of NES-Leu11/Ile13 as well as the backbone amide of NES-Asp12, illustrated by red dashed lines) is consistent with an equivalent hydrogen bonding network in the PKI Φ^0Leu NES·CRM1·RanGTP complex.

(d) Binding of the indicated CRM1 variants to the specified export ligands. Changing CRM1-Cys528 to other small residues with hydrophobic potential (Ala, Thr, Val) did not reduce cargo binding detectably. A change to the more hydrophilic Ser, however, caused some reduction and a change to the bulky residue Trp resulted in a clear decrease in cargo binding. See **Figure 2e** for further details. These results confirm that PKI and Rev NES bind in close vicinity of CRM1-Cys528 and CRM1-Ala541. See also **Supplementary Figure 1** and **2**.

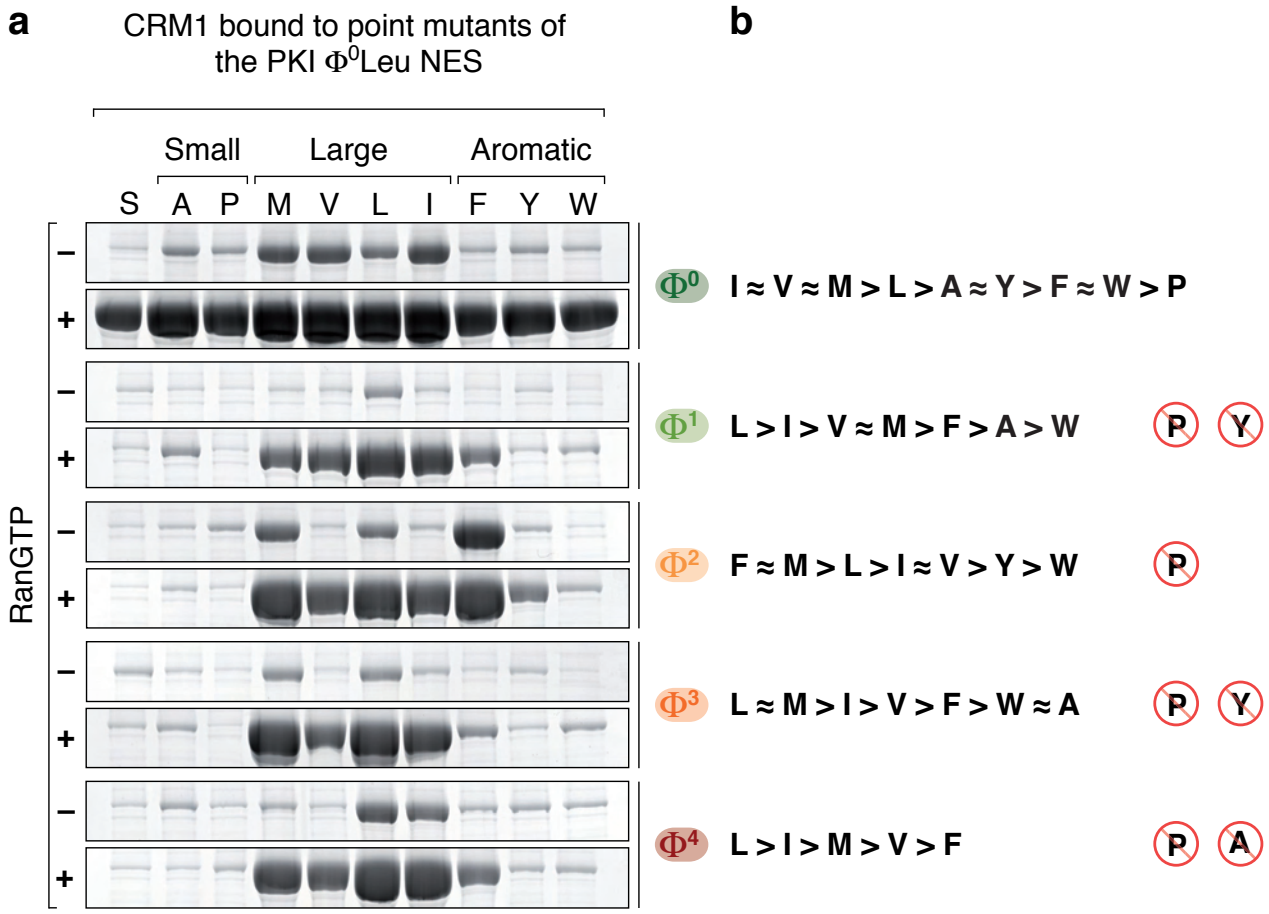

Supplementary Figure 6 Assessment of the amino acid specificities of the Φ pockets (related to **Figs. 4, 8**).

(a) Each Φ residue of the zz-tagged PKI Φ^{0}Leu NES was systematically mutated to the indicated hydrophobic residues (single letter codes) and tested for CRM1 binding in the absence or presence of RanGTP as described for **Figure 4a**. Ser mutants were used as negative controls, because Ser should not engage in hydrophobic interactions with Φ pockets. We considered residues as clearly Φ-active if (i) CRM1 recruitment to the mutant peptide was stimulated by RanGTP and (ii) if CRM1 binding was more pronounced than for the corresponding Ser mutant. Substitutions that reduced bound CRM1 to background levels can be regarded as disallowed.

(b) Panel shows the NES consensus derived from **a** and **Figure 4c** (see also **Fig. 8**).

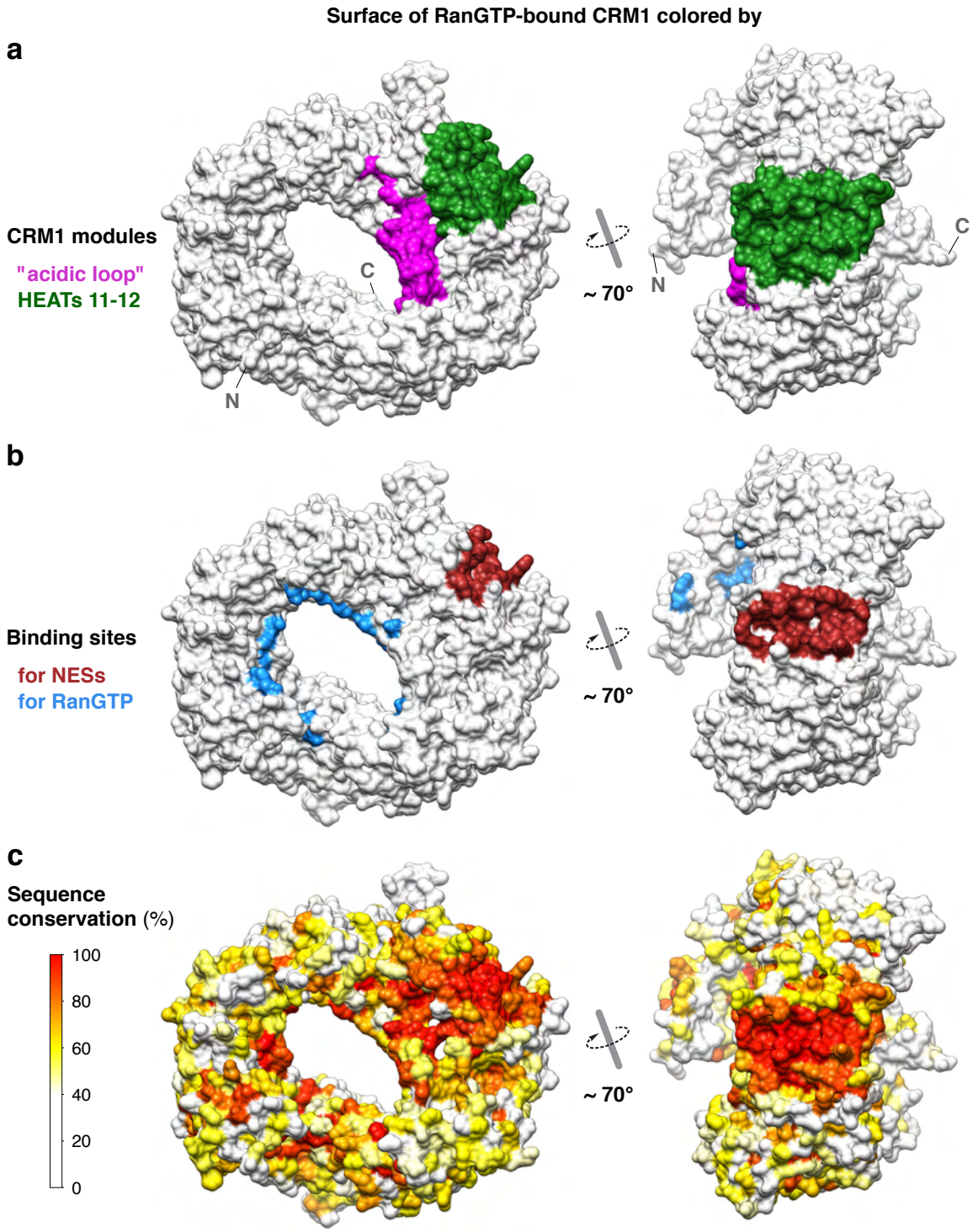

Supplementary Figure 7 Sequence conservation of CRM1.
CRM1 (in export complex conformation) is shown as a surface representation, ligands have been omitted for clarity.
(a) The "acidic loop" (residues 423-448) is colored in magenta, HEAT repeats 11 and 12 (residues 510-595) in green. The locations of N- and C-terminus are shown for orientation.
(b) The Ran-binding surface is depicted in blue and the NES-binding surface is shown in brown.
(c) CRM1 surface is colored according to sequence conservation. Note that the NES-binding site is the most conserved part of CRM1. Striking conservation further extends to the acidic loop that links Ran- and NES-binding. The surface representation was generated with UCSF Chimera[2] from Clustal W[3]-aligned CRM1 sequences. The alignment was essentially based on all full-length CRM1 sequences that were identifiable in the non-redundant NCBI protein sequence database, the most distant being CRM1 from *Trichomonas vaginalis* (22 % identity to mouse CRM1). For sets of highly similar sequences however, only one orthologue was included in order to avoid bias by overrepresenting individual clades, leaving 58 sequences.

Supplementary Table 1 Crystallization and cryoprotection conditions.
(related to **Figs. 2**, **7** and **Supplementary Figs. 1-3, 5**)

Complex	Crystallization		Cryoprotection
PKI Φ^{0}Leu NES-SPN1·CRM1·Ran (res. 5-180; Q69L)	100 mM Tris/HCl pH 8.08-8.30, 10-14% (w/v) PEG 1000 **(20 °C)**	sitting drop 1 µl prot. (4 mg ml^{-1}) + 1 µl reservoir	reservoir + 20% (v/v) 1,2-propanediol
HIV-1 Rev NES-SPN1·CRM1·Ran (res. 5-180; Q69L) *crystal I*	100 mM Tris/HCl pH 7.8, 16% (w/v) PEG 1000 **(16 °C)**	hanging drop 2 µl prot. (8 mg ml^{-1}) + 2 µl reservoir	reservoir + 5% (w/v) PEG 1000 + 12% (v/v) glycerol
HIV-1 Rev NES-SPN1·CRM1·Ran (res. 5-180; Q69L) *crystal II*	100 mM Tris/HCl pH 7.8, 16% (w/v) PEG 1000, 2 mM phenol **(20 °C)**	hanging drop 2 µl prot. (8 mg ml^{-1}) + 2 µl reservoir	reservoir + 5% (w/v) PEG 1000 + 12% (v/v) glycerol
CRM1·Ran (res. 1-180; Q69L)	100 mM Tris/HCl pH 8.5, 12% (w/v) PEG 4000 **(20→4 °C)**	sitting drop 1 µl prot. (12.2 mg ml^{-1}) + 1 µl reservoir	reservoir + 11% (v/v) 2,3-butanediol

Supplementary Methods

Protein expression and purification

2YT medium supplemented with 2% (w/v) glycerol and 30 mM K_2HPO_4 was used for standard expression cultures. Mouse CRM1 (full-length, residues 1-1071) was expressed as an N-terminal His_{10}-zz fusion in *E. coli* BLR using a fermenter (Labfors 3, Infors AG). Expression was performed at 16 °C for ≈ 20 hours (0.1 mM IPTG). A total of 1 mM PMSF and 1 mM EDTA were added to the culture prior to centrifugation. Cells were resuspended in lysis buffer (50 mM Tris/HCl pH 7.5, 500 mM NaCl, 1 mM EDTA, 2 mM imidazole) supplemented with 100 μM Amidino-PMSF and 100 μM DFP and lysed in the presence of 5 mM DTT and 20 U ml^{-1} Benzonase (Novagen). The lysate was cleared by centrifugation and the protein bound to a Ni^{2+}-chelate affinity column. To remove CRM1-associated chaperones, the column was washed with lysis buffer supplemented with 100 mM KCl, 10 mM $Mg(OAc)_2$ and 1 mM ATP. CRM1 was eluted with lysis buffer/200 mM imidazole. The eluate (diluted to 100 mM NaCl) was passed through a Heparin Sepharose column (GE Healthcare), applied to a Q-Sepharose column (GE Healthcare) and eluted in a concentration gradient of NaCl. After cleavage of the His_{10}-zz-tag by His-tagged TEV protease, the tag, protease and residual contaminants were removed via another Ni^{2+}-column. The flow-through was then subjected to a Superdex 200 gel filtration column (HiLoad 26/60, GE Healthcare, equilibrated in 50 mM Tris/HCl pH 7.5, 500 mM NaCl, 2 mM $Mg(OAc)_2$, 1 mM EDTA, 5 mM DTT).

We truncated the C-terminus of Ran, since it is disordered in other transport receptor complexes[4,5], it destabilizes the GTP-bound form of Ran and counteracts the interactions with transport receptors[6]. Human Ran Q69L (residues 1-180) and Ran Q69L (residues 5-180) were expressed as an N-terminal His_{10}-zz fusion in *E. coli* BLR (0.1 mM IPTG for ≈ 16 hours at 20 °C). Protease inhibitors were applied as described for CRM1. Cells were lysed in 50 mM K-Phosphate pH 7.0, 500 mM NaCl, 5 mM $Mg(OAc)_2$, 1 mM EDTA, 2 mM imidazole, 2 mM DTT (lysis buffer). The protein was purified by Ni^{2+}-chelate affinity chromatography. 20 μM GTP were included in all buffers subsequent to cell lysis. The His_{10}-zz tag was cleaved off by TEV protease during dialysis of the Ni^{2+}-eluate to lysis buffer. The flow-through of a second Ni^{2+}-column was further purified by gel filtration chromatography (HiLoad 26/60 Superdex 200, GE Healthcare, equilibrated in 50 mM K-Phosphate pH 7.0, 500 mM NaCl, 5 mM $Mg(OAc)_2$, 1 mM EDTA, 2 mM DTT). To confirm the nucleotide state of Ran, the nucleotide was dissociated from the protein by addition of de-ionized urea and the nucleotide pattern analyzed by anion exchange chromatography on a MonoQ 5/50 GL column (GE Healthcare).

All human SPN1 and SPN1-derived constructs, i.e. full-length SPN1 (residues 1-360), the NES-SPN1 chimeras (SPN1 residues 15-360) and SPN1 ΔN were expressed as N-terminal His_{10}-zz fusions in *E. coli*

Nature Structural & Molecular Biology: doi:10.1038/nsmb.1931

BLR (0.1 mM IPTG for ≈ 16 hours at 18 °C). Protease inhibitors were applied as described for CRM1. Cells were lysed in 50 mM Tris/HCl pH 7.5, 200 mM NaCl, 2 mM $Mg(OAc)_2$, 1 mM EDTA, 2 mM imidazole, 5 mM DTT (lysis buffer). The protein was purified by Ni^{2+}-chelate affinity chromatography. The eluate (diluted to 50 mM NaCl) was bound to a Q-Sepharose column (GE Healthcare) and eluted in a concentration gradient of NaCl. After cleavage of the His_{10}-zz tag by His-tagged TEV protease, the protein was passed over a second Ni^{2+}-chelate affinity column and polished by gel filtration (HiLoad 26/60 Superdex 200, GE Healthcare, equilibrated in 50 mM Tris/HCl pH 7.5, 200 mM NaCl, 2 mM $Mg(OAc)_2$, 1 mM EDTA, 5 mM DTT).

His_{10}-zz-tagged NES peptides (PKI NES: *Homo sapiens*, Rev NES: HIV-1, NS2 NES: Minute Virus of Mice, An3 NES: *Xenopus laevis*, S1: synthetic) were expressed in *E. coli* BLR (1 mM IPTG for ≈ 5 hours at 37 °C) and purified under denaturing conditions (lysis buffer: 50 mM Tris/HCl pH 8.0, 6 M guanidinium hydrochloride, 1 mM EDTA, 5 mM DTT) by Ni^{2+}-chelate affinity chromatography (elution in 50 mM Tris/HCl pH 7.5, 8 M urea, 50 mM NaCl, 200 mM imidazole, 1 mM EDTA, 5 mM DTT), followed by dialysis to 50 mM Tris/HCl pH 7.5, 50 mM NaCl, 2 mM $Mg(OAc)_2$, 2 mM DTT for refolding. The His_{10}-zz tag used as a control in binding assays (**Figs. 6a** and **7d**) was obtained by TEV protease cleavage of an NES fusion construct. His_{10}-zz-tagged human Ran Q69L (residues 1-180; **Fig. 1b**) was prepared according to the Ran preparation procedure described above. All CRM1 forms used for **Figure 2e** and **Supplementary Figure 5d** were expressed as N-terminal His fusions (as described for CRM1, see above) and purified by Ni^{2+}-chelate affinity chromatography.

eGFP-spacer-NES fusions (N-terminally His_{10}-tagged, C-terminal Cys) were expressed in *E. coli* TOP10F' (0.2 mM IPTG for ≈ 16 hours at 18 °C) and bound to a Ni^{2+}-chelate affinity column (lysis buffer: 50 mM K-Phosphate pH 7.0, 200 mM NaCl, 2 mM $Mg(OAc)_2$, 1 mM EDTA, 2 mM imidazole, 5 mM DTT). The proteins were direcly eluted onto a home-made thiopyridine-activated, SH-reactive Sepharose matrix (pH adjusted to 7.5) to select for full-length NES species. Elution from SH-Sepharose was performed with lysis buffer (pH adjusted to 7.5, supplemented with 5 mM DTT). The eluate was dialyzed to 50 mM Tris/HCl pH 7.5, 100 mM NaCl, 2 mM $Mg(OAc)_2$, 2 mM DTT. mCherry and PKI Φ^0Leu NES-mCherry (TEV protease-cleavable His_{14}-fusions) were expressed and purified following the procedure described for mCherry[7].

To obtain NMR spectra of good quality, uniform deuteration of CRM1 was essential. For this, we optimized the fully deuterated minimal medium to support robust expression of CRM1 and cell growth to high optical densities (OD_{600} 6-10, manuscript in preparation). CRM1 expression was induced with 0.05 mM IPTG for nine (!) days at 16 °C. Purification of deuterated CRM1 followed the procedure described for the non-deuterated protein. The His_{10}-zz-tagged PKI Φ^0Leu NES was produced with various methyl-protonation

Nature Structural & Molecular Biology: doi:10.1038/nsmb.1931

schemes[8,9] and purified as described for the unlabeled peptide fusion constructs. The tag was cleaved off by TEV protease and removed via a Ni^{2+}-column. The peptide was then loaded onto a reversed-phase HPLC column (C-18, 218TP1022, GraceVydac), eluted by increasing the concentration of acetonitrile in the presence of 0.5% (v/v) TFA, and lyophilized.

Protein sample preparation for crystallization and NMR analysis

For crystallization, complexes were reconstituted in 20 mM Tris/HCl pH 7.5, 50 mM NaCl, 2 mM $Mg(OAc)_2$, 5 mM DTT as described[1].

Samples for NMR spectroscopy were prepared by mixing the NES peptide, CRM1 and Ran Q69L (residues 5-180) in a 1:1.4:1.4 ratio, followed by dialysis against 20 mM Na-Phosphate pH 6.8, 50 mM NaCl, 2 mM $MgCl_2$, 5 mM DTT, 30 μM GTP and concentration to 0.1-0.2 mM (export complex). NMR spectra of the free NES were recorded at 1 mM peptide concentration.

NMR assignment

Conventional TROSY versions of triple resonance experiments failed for the bound PKI NES residues in the complex. This is due to the relatively low concentrations around 0.1-0.2 mM (limited by the solubility of the protein complex) and the adverse relaxation properties that reflect the size of the complex (calculated correlation time: 90 ns (HYDRONMR[10]). Sample stability further limited NMR measurements to ambient temperature. Resonance assignment was carried out using several specifically isotope labeled samples, namely [U-^{2}H, ^{15}N, ^{13}C, I/L/V ^{1}H, ^{13}C-methyl] and [U-^{2}H, ^{15}N, ^{13}C, Ala-^{1}H, Leu/Val ^{1}H, ^{13}C-methyl] PKI NES, respectively. Unique amino acids (e.g. Ile13) were used as starting points for the resonance assignment in ^{13}C/^{15}N edited NOESY-HMQC experiments acquired at different mixing times. Two continuous methyl-walks involved residues Leu1, Leu4 and Leu8, Leu11, Ile13, respectively. For one leucine methyl group (Leu6), no NOE cross peaks to any other methyl groups were observed.

As the standard route towards backbone dihedral angle restraints from ^{13}C chemical shifts[11] via conventional TROSY versions of triple resonance experiments failed, we used ^{13}C direct-detected experiments to assign backbone ^{13}Cα and side chain ^{13}C chemical shifts. A combination of ^{13}C-^{13}C TOCSY and ^{13}C-^{13}C NOESY experiments provided complementary chemical shift data. Whereas cross peaks for residues located within the flexible termini of the PKI NES peptide were observed in the ^{13}C-^{13}C TOCSY experiment, the ^{13}C-^{13}C NOESY provided chemical shifts for the CRM1-bound residues that tumble with the correlation time of the complex. The efficiency of the dipolar transfer between ^{13}C spins increases with the correlation time[12], and

Nature Structural & Molecular Biology: doi:10.1038/nsmb.1931

thus, residues located within the flexible termini did not give rise to detectable cross peaks at the used mixing times of 500 ms. The ^{13}C-^{13}C NOESY yields cross peaks exclusively for the directly bonded carbons. This is due to the generally much shorter distances between directly bonded carbon and the strong (r^{-6}) distance dependency of the dipolar transfer. ^{13}C chemical shifts of leucine and isoleucine methyl groups were used as starting point for the ^{13}C resonance assignment. The remaining amino acids were assigned based on their characteristic ^{13}C chemical shifts and spin systems. ^{13}Cα and ^{13}Cβ chemical shifts were then used as input to derive backbone dihedral angle restraints[11]. Further details of the assignments and structure calculation will be described in a manuscript by T. Madl et al. (in preparation).

Crystallization of the RanGTP·CRM1 complex

The crystallization of the binary CRM1·RanGTP complex was initially started with a ternary PKI Φ^{0}Leu NES·CRM1·RanGTP complex (with the NES not fused to the SPN1 module). However, crystal growth was most probably initiated only after a contaminating bacterial protease had removed the NES peptide as well as 21 residues from the C-terminus of CRM1. This interpretation is supported by the following observations: (i) Crystals were observed only after more than five months. (ii) After this time, CRM1 in the used protein preparation was found to be quantitatively cleaved. (iii) More highly purified, protease-free preparations of the intact ternary complex were fully refractory to crystallization. (iv) The structure of CRM1 in the obtained crystals is clearly defined up to His1050, whereas the complete C-terminus (ending at residue 1071) can probably not be accommodated into the observed crystal lattice. And (v) no electron density for an NES peptide was traceable. See also **Table 1** and **Supplementary Table 1**.

Software used for preparation of figures

Structural representations have been generated with PyMOL (http://www.pymol.org) and, where indicated, with UCSF Chimera[2]. Figures were prepared using Photoshop and Illustrator (Adobe Systems Inc.).

Nature Structural & Molecular Biology: doi:10.1038/nsmb.1931

Supplementary References

1. Monecke, T. et al. Crystal structure of the nuclear export receptor CRM1 in complex with Snurportin1 and RanGTP. *Science* **324**, 1087-1091 (2009).

2. Pettersen, E. F. et al. UCSF Chimera--a visualization system for exploratory research and analysis. *J Comput Chem* **25**, 1605-1612 (2004).

3. Larkin, M. A. et al. Clustal W and Clustal X version 2.0. *Bioinformatics* **23**, 2947-2948 (2007).

4. Vetter, I. R., Arndt, A., Kutay, U., Görlich, D. & Wittinghofer, A. Structural view of the Ran-Importin beta interaction at 2.3 A resolution. *Cell* **97**, 635-646 (1999).

5. Cook, A., Bono, F., Jinek, M. & Conti, E. Structural biology of nucleocytoplasmic transport. *Annu Rev Biochem* **76**, 647-671 (2007).

6. Richards, S. A., Lounsbury, K. M. & Macara, I. G. The C terminus of the nuclear RAN/TC4 GTPase stabilizes the GDP-bound state and mediates interactions with RCC1, RAN-GAP, and HTF9A/RANBP1. *J Biol Chem* **270**, 14405-14411 (1995).

7. Frey, S. & Görlich, D. FG/FxFG as well as GLFG repeats form a selective permeability barrier with self-healing properties. *EMBO J* **28**, 2554-2567 (2009).

8. Gardner, K. H. & Kay, L. E. The use of 2H, 13C, 15N multidimensional NMR to study the structure and dynamics of proteins. *Annu Rev Biophys Biomol Struct* **27**, 357-406 (1998).

9. Tugarinov, V., Kanelis, V. & Kay, L. E. Isotope labeling strategies for the study of high-molecular-weight proteins by solution NMR spectroscopy. *Nat Protoc* **1**, 749-754 (2006).

10. García de la Torre, J., Huertas, M. L. & Carrasco, B. HYDRONMR: prediction of NMR relaxation of globular proteins from atomic-level structures and hydrodynamic calculations. *J Magn Reson* **147**, 138-146 (2000).

11. Shen, Y., Delaglio, F., Cornilescu, G. & Bax, A. TALOS+: a hybrid method for predicting protein backbone torsion angles from NMR chemical shifts. *J Biomol NMR* **44**, 213-223 (2009).

12. Fischer, M. W. F., Zeng, L. & Zuiderweg, E. R. P. Use of C-13-C-13 NOE for the assignment of NMR lines of larger labeled proteins at larger magnetic fields. *J Am Chem Soc* **118**, 12457-12458 (1996).